Spectrochimica Acta Part A: Molecular and Biomolecular Spectroscopy 170 (2017) 145–149

Contents lists available at ScienceDirect

Spectrochimica Acta Part A: Molecular and Biomolecular Spectroscopy

journal homepage: www.elsevier.com/locate/saa

Mid infrared emission spectroscopy of carbon plasma

Laszlo Nemes [a,*], Ei Ei Brown [b], Clayton S.-C. Yang [c], Uwe Hommerich [b]

[a] Research Center for Natural Sciences, Hungarian Academy of Sciences, Budapest 1519, Hungary
[b] Department of Physics, Hampton University, Hampton, Virginia 23668, USA
[c] Battelle Eastern Sciences and Technology Center, Aberdeen, MD 21001, USA

ARTICLE INFO

Article history:
Received 13 January 2016
Accepted 28 June 2016
Available online 30 June 2016

Keywords:
LIBS
Plasma
Carbon
Cluster
Infrared
Emission

ABSTRACT

Mid infrared time-resolved emission spectra were recorded from laser-induced carbon plasma. These spectra constitute the first study of carbon materials LIB spectroscopy in the mid infrared range. The carbon plasma was induced using a Q-switched Nd: YAG laser. The laser beam was focused to high purity graphite pellets mounted on a translation stage. Mid infrared emission from the plasma in an atmospheric pressure background gas was detected by a cooled HgCdTe detector in the range 4.4–11.6 μm, using long-pass filters. LIB spectra were taken in argon, helium and also in air. Despite a gate delay of 10 μs was used there were strong backgrounds in the spectra. Superimposed on this background broad and noisy emission bands were observed, the form and position of which depended somewhat on the ambient gas. The spectra were digitally smoothed and background corrected. In argon, for instance, strong bands were observed around 4.8, 6.0 and 7.5 μm. Using atomic spectral data by NIST it could be concluded that carbon, argon, helium and nitrogen lines from neutral and ionized atoms are very weak in this spectral region. The width of the infrared bands supports molecular origin. The infrared emission bands were thus compared to vibrational features of carbon molecules (excluding C_2) of various sizes on the basis of previous carbon cluster infrared absorption and emission spectroscopic analyses in the literature and quantum chemical calculations. Some general considerations are given about the present results.

1. Introduction

Infrared absorption spectroscopy has been the mainstay in chemical structural analysis since a long time. Infrared emission has also been harnessed in chemistry, physics and especially in astronomy to study molecules in terrestrial and cosmic sources. Very good treatises may be found in the literature summarizing principles and applications of infrared emission spectroscopy [1–3]. In the past two decades Fourier transform spectroscopic methods have been extended to time-resolved studies of infrared emission (e.g. in plasma analysis [4]). This method however requires complicated equipment and has not been adopted on a large scale, especially not for field applications.

Following the initiatives of Alan C. Samuels at the Edgewood Chemical Biology Center between 2000 and 2002, in the past decade a new approach has been elaborated for the study of infrared emission spectroscopy from laser-induced breakdown (LIBS) plasmas [5–11]. The use of fast and sensitive cooled photo-conductive detectors such as InSb and HgCdTe (MCT) made it possible to apply this direct detection method for stand-off field analysis of various materials using relatively simple optical constructs.

The main advantage of using infrared methods in LIBS analyses over traditional visible/UV spectroscopy is that molecular vibrational features may be observed. In conventional LIB spectroscopy electronic transitions are detected only up to a maximum of triatomic molecules. In the mid infrared (fingerprint) region on the other hand vibrational spectra of all molecules that posses infrared active vibrations are routinely found.

The science of carbon had a 'renaissance' following the chemical Nobel Prize winning (1996) discovery of the fullerenes in 1985 and their macroscopic preparation five years later [12–14]. A huge number of papers have been published in the following years on fullerenes and other carbon clusters. The size of this literature is far too large to reference it here. Some aspects of the field are surveyed in a review book published five years ago [15]. Conventional UV/visible LIBS analyses carried out for carbon plasmas so far have not yielded proof for the existence of large carbon molecules (the largest detected so far being the C_3 radical). Laboratory observation of larger carbon molecules in plasmas are of direct interest to nanomaterial science and infrared astronomy [16,17]. We have undertaken an exploratory study of mid infrared emission spectra obtained from laser generated carbon plasmas and report the results here. To our knowledge this is the first such study in the literature.

* Corresponding author.
E-mail addresses: nemesl@comunique.hu (L. Nemes), eiei.nyein@hampton.edu (E.E. Brown), yangc@battelle.org (C. S.-C. Yang), uwe.hommerich@hampton.edu (U. Hommerich).

http://dx.doi.org/10.1016/j.saa.2016.06.046
1386-1425/

2. Experimental

The measurements were conducted at pump energy of ~50 mJ using an actively Q-switched Nd:YAG pulsed laser (1064 nm) with 5 ns pulse width, 10 Hz repetition rate. The laser beam was focused with a lens (focal length = 5 cm) onto a high purity graphite pellet cut from rods (NAC Carbon Products: NAC-500 extruded graphite rod) leading to a beam diameter of ~0.2 mm (fluence ≈ 40 J/cm^2). The pellet was affixed to a linear translation stage controlled by a stepper motor using motion controller. The stage was translated at a speed of about 1 mm/min to provide fresh surfaces for subsequent laser pulses. Two ZnSe lenses (focal length = 10 cm) were employed as collection optics to focus the infrared emission onto the entrance slit of a 0.15 m spectrometer. The emission was dispersed using a grating blazed at 8 μm and a liquid nitrogen cooled single element MCT detector for detection in the 8–12 μm region (then between 4.5 and 12 μm). Scattered laser light and higher order spectra were removed by low-pass filters cutting at 4 and 7.4 μm. The entrance and exit slits of the spectrometer were 2 mm wide. The spectral resolution was about 80 nm. The spectral range above was scanned at intervals 4400–5600, 5600–6800, 6800–8000, 8000–9200, 9200–10,400 and 10,400–11,600 nm using scanning speed 100 nm/min. The total scan was around 1 h. After one scan the sample mount was laterally displaced so that the next scan had new surface. Signals from ten spectra were averaged using a boxcar with 10 μs delay and 16 μs gate-width.

The infrared LIBS apparatus was placed in a plastic box taped up to stop environmental air and humidity getting into the box. The whole volume was purged, for instance, by ultra-pure grade 5.0 argon gas. Twenty minutes purging time was allowed before starting the LIBS measurements. Fig. 1 shows the experimental setup of the mid IR LIBS emission.

3. Spectra

Figs. 2–4 show raw spectra using helium, argon or air as background gases in the wavelength range 8–11.5 μm. The room temperature spectrometer background was obtained by recording emission from the spectrometer housing in the absence of the laser impulses. This background can be safely ignored as it is almost flat and nearly zero throughout the spectral range.

Fig. 5 shows a processed spectrum between 8 and 11.5 μm in helium.

Processed spectra were obtained from the raw experimental spectra in Figs. 2–4 via a de-noising process using the astronomy software SPLAT from the website given in [18].

Using SPLAT one is able to apply various filters to re-bin or average a spectrum and correct for backgrounds. In Fig. 5, a Welch window was used that removed most of the noise and suppressed 'channelling' (interference fringes) arising from the presence of the long pass laser-light filter (see Fig. 1).

The spectral background in Figs. 2–4 increasing towards higher energies was fitted by a third-order polynomial and subtracted from the spectrum. (In Fig. 4 the spectrum in air was so much overlapped by the instrument background that processing was abandonEd.) Possible sources for this background are discussed in Section 4. The correction for relative intensity effects due to the instrumental transfer function was neglected as we were not studying intensities. A similar processed spectrum taken in argon in the same spectral range is shown in Fig. 6.

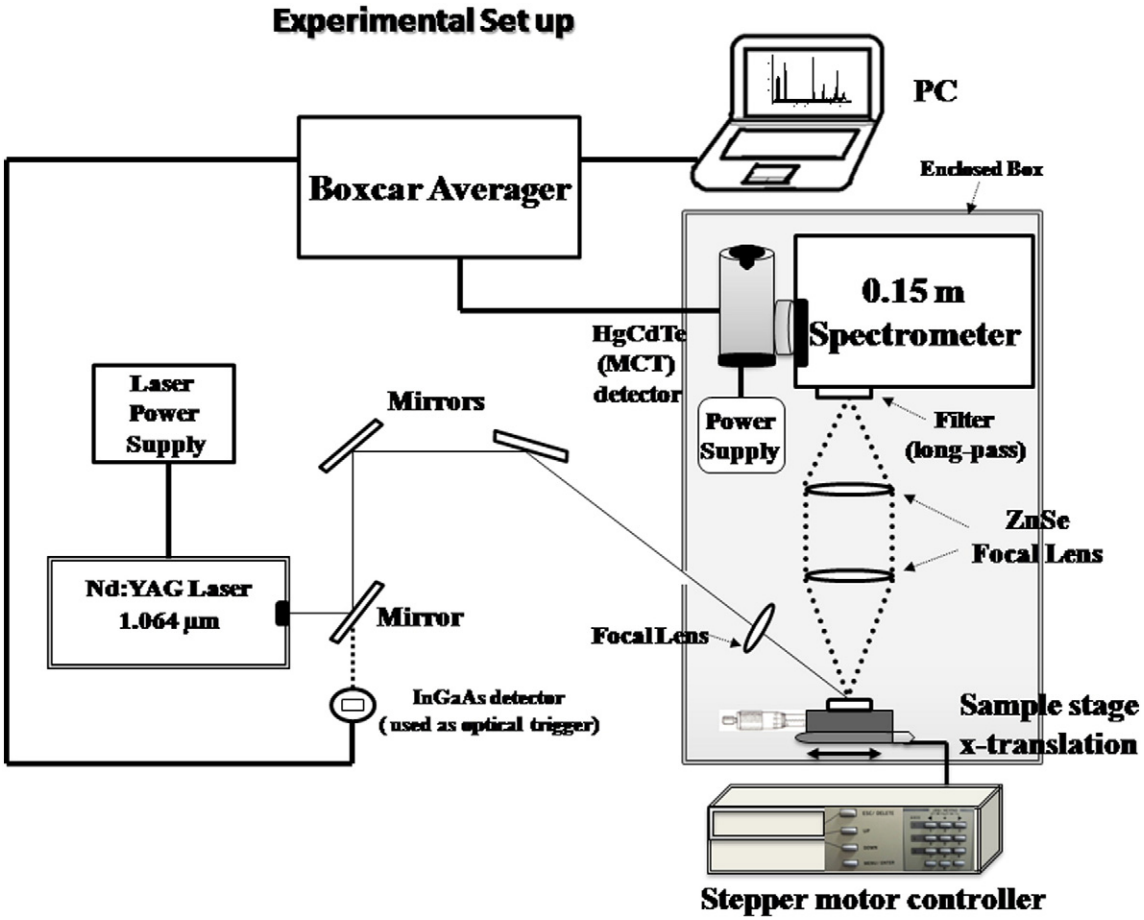

Fig. 1. Schematic diagram of the experimental setup for the infrared LIBS emission.

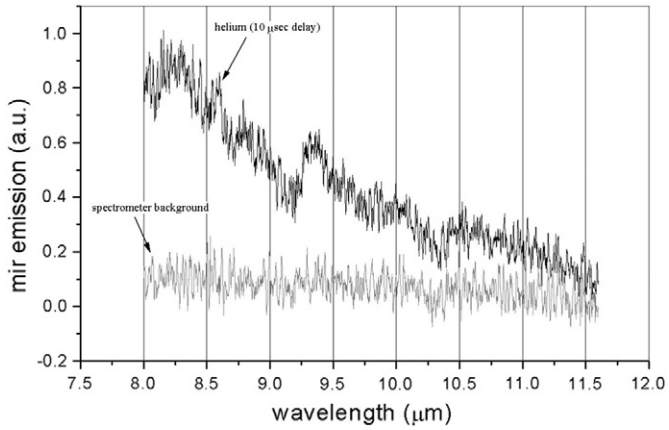

Fig. 2. Raw spectrum in helium, instrument background in gray.

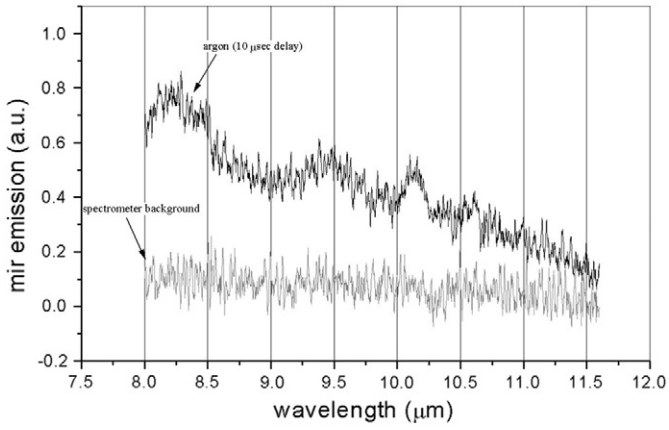

Fig. 3. Raw spectrum in argon, instrument background in gray.

Fig. 7 presents another processed spectrum in argon taken over a broader spectral range 4.4–11.5 μm.

4. Discussion of spectral assignments

The present infrared emission spectra are significantly different from those previously reported [5–11]. Apart from graphitic carbon atom sheets, in the present experiments there are no target molecules available before the laser hits the sample surface so no existing molecules are desorbed by thermal effects. Impurities in the graphite sample are negligible. Thus any molecules observed must arise in the plasma and/or from laser ablation of graphite.

Before a molecular interpretation of the present spectra is attempted one must inquire whether the features observed are due to electronic transitions of carbon, argon, helium or nitrogen atoms. The NIST atomic database (ASD) [19] contains mid infrared lines for neutral carbon and its ionic forms.[1] The database also contains Ritz combination wavelengths calculated from energy levels. The ASD provides Saha-LTE relative intensity spectral plots (at local thermal equilibrium) that help identifying lines. Similar plots are available also for neutral and ionized Ar, He, and N. In order to generate such plots one needs input values for the electron temperature, ion temperature (for ion lines) and electron density values. As such values were not available from the present experiments (see the end of this section) we have used estimates of electron temperature $T_e = 1$ eV (11,600 K), ion temperature $T_i = 78{,}000$ eV and electron number density $N_e = 1 \times 10^{19}$ cm^{-3} (see Footnote 1). The very high ion temperature used is unphysical and was only intended to induce some thermal (Doppler) line broadening for the lines rendering spectral plots more realistic.

These ASD plots indicate that, based on presently available data, ionized carbon lines are of negligible intensity in our spectral range, while the only neutral carbon line of significant intensity occurs near 4.59 μm. As this line has not yet been observed, the ASD data are based on Ritz combinations. Similarly Ar, He and N and their ionic forms either have no observed electric dipole lines or only very weak such lines in our mid infrared range. First ionized argon does have a magnetic dipole transition at 6.98 μm, but this is electric dipole forbidden so cannot appear in our spectra.

In carbon vapours and plasmas the so-called Swan electronic bands of the C_2 radical are always observed [20]. C_2, however, is invisible in the mid infrared range, as it is a homopolar molecule thus its vibrational transitions are electric dipole forbidden. Heavier carbon chains can be detected as their infrared vibration spectra always contain infrared active $\sigma(u)$ modes [21]. The C_3 radical is known to be the most abundant linear chain in equilibrium carbon vapours and it is also found by laser-induced-fluorescence methods in carbon plasmas [16]. Its ν_3 antisymmetric stretching mode falls to 4.9 μm (2040 cm^{-1}) within the strong band we observed in our plasma between 4.4 and 5.4 μm (see Fig. 7).[2] Table 1 contains C_5, C_6, C_7 and C_9 molecules that have IR active modes at 4.6, 5.1, 4.7 and 4.8 μm, respectively.

Thus it is very likely that we have detected C_3 and some higher chain analogues in our spectra. The most intense band in Fig. 7 is found at 7.3–7.5 μm and a band of medium intensity is located near 6 μm. Perhaps the most intriguing possibility is the emergence of fullerenes C_{60} and C_{70} in our plasma spectra. There are a number of papers dealing with infrared spectra of solid phase fullerenes [13,22] and there are two papers on the gas-phase thermal infrared emission spectra of these large clusters [23,24]. It appears reasonable to compare our plasma spectrum to that of gas-phase fullerenes. A spectral comparison (Fig. 8) shows the infrared gas-phase emission spectrum of C_{60} taken from [24] superimposed on our argon spectrum taken from Fig. 7.

The FTIR spectrum shown in gray indicates two strong bands of C_{60} at 7.1 and 8.5 μm corresponding to ν_{25} and ν_{26}, respectively. The temperature of the carbon gas was 960 K (687 °C).

The strong emission in our spectrum at around 7.4 μm overlaps ν_{25} of C_{60}, while the medium weak feature between 8 and 8.5 μm in Fig. 7 falls to the shorter wavelength side of the ν_{26} of C_{60} at about 8.47 μm. This corresponds to about 5 cm^{-1} difference. In [24] the temperature shifts of the four infrared bands of C_{60} were estimated. For the ν_{26} band this shift amounts to about -0.02 cm^{-1} per Kelvin. Thus if the temperature of C_{60} would be about 700 K (450 °C) its ν_{26} band would appear roughly at the position of the small peak at 8.47 μm in Fig. 7. The intensity of this band suggests that the quantity of C_{60} is rather small in our spectrum. Thus although we have presently no conclusive proof, is not excluded that we have weak C_{60} features in our spectra. It is well known that carbon plasma generation in the presence of rare gases leads to fullerene formation [12,13].

Apart from the above considerations the strong 7.4 μm feature in Fig. 7 must contain vibration(s) of other carbon cluster(s). Also the medium strong band at 6 μm cannot correspond to either C_{60} or C_{70} or linear carbon chains thus other molecular assignments should be sought after.

In the course of laser ablation of graphite in our experiments graphitic layer fragments may appear. These are essentially dehydrogenated polycyclic aromatic hydrocarbons (dPAH molecules). While the experimental and theoretical spectroscopic literature on PAHs is very extensive, as these molecules are of great astrophysical/astrochemical significance [25] only theoretical vibrational spectroscopic data from quantum chemical (density functional) calculations are available on dehydrogenated PAH molecules [26]. These calculations

[1] The authors are indebted to Dr. Alexander Kramida at NIST for pointing out several features of ASD in connection with carbon, argon and helium mid infrared lines.

[2] We have not attempted to fit Gaussian or Lorentzian profiles to our bands as their structure is complicated thus is it uncertain how many components are contained in their envelopes.

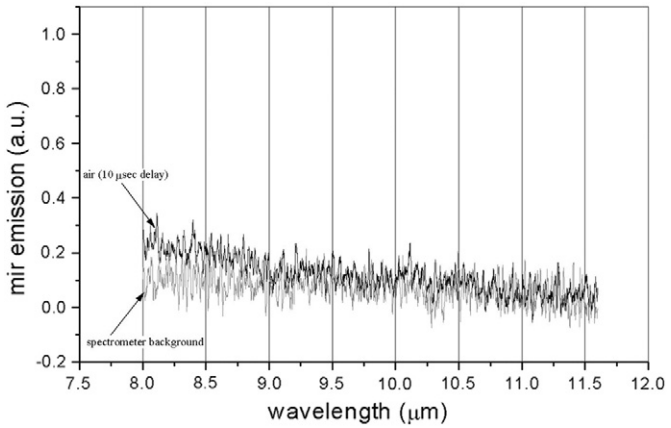

Fig. 4. Raw spectrum in air, instrument background in gray.

show that the strongest dPAH infrared transitions occur in two groups, one between 5 and 12 μm and another between 17 and 28 μm, yielding the highest density of transitions around 7, 11 and 18 μm. Thus the strong emission feature between 7.3 and 7.4 μm in Fig. 6 may contain dPAH infrared bands.

It is also interesting to compare our spectra in Figs. 5 and 6 that demonstrate differences between helium and argon atmospheres. For example there is a large difference around 10.2 μm. In general the two spectra are rather dissimilar so the two kinds of plasmas have somewhat different chemical constitution. So the formation of carbon molecules (clusters) yields different structures when the background rare gas is changed. The spectral range at lower wavelengths in argon (between 4.4 and 8 μm) - see Fig. 7 - contains much stronger bands than between 8 and 11.5 μm. We do not presently have a corresponding comparison in helium atmosphere.

Rare gases are much more productive in cluster formation than N_2. This is demonstrated by Fig. 4 that shows a spectrum taken in air. In this background gas infrared bands are much weaker than either in argon or helium. Another interesting property of our mid infrared emission spectra is the strong background (see Figs. 2 and 3), Figs. 5–8 are already corrected for this background. As the gate delay used in our spectra was 10 μs this background could not originate from plasma continuum radiation, as that lasts only a few hundred nanosecond and thus gated out from our spectra.

Due to the near perfect absorption of infrared by the black carbon material it may be heated significantly when the laser strikes the graphite sample. The cooling of the sample surface takes much longer than plasma continuum radiation and may be the source of a thermal signature in our spectra. In fact, noting that this background does not appear

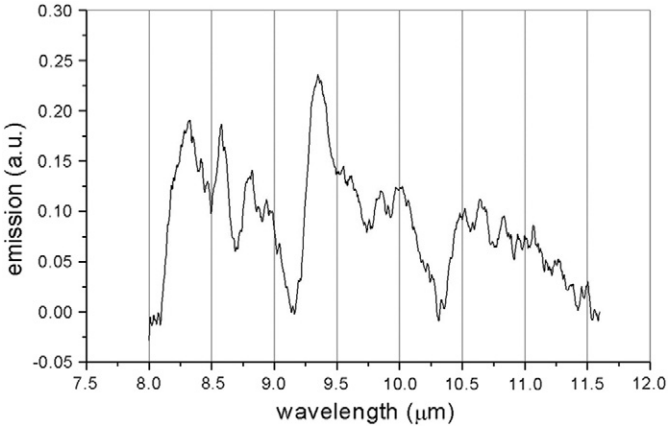

Fig. 5. Carbon plasma spectrum in helium, noise-filtered by a Welch filter, and spectral background corrected using 3rd-order polynomial fit to the base of the raw spectrum.

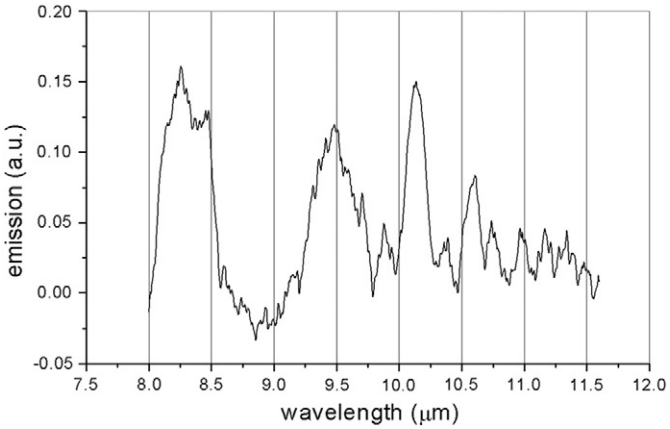

Fig. 6. Carbon plasma spectrum in argon between 8 and 11.5 μm, noise-filtered by a Welch filter, and spectral background corrected using 3rd-order polynomial fit to the base of the raw spectrum.

to have a maximum in the spectral range we study it should correspond to the long wavelength slope of the Planck curve. As a background maximum is not observed above 4.4 μm in cubic polynomial fits to the base line in our spectra it is not possible to fit the background to a Planck curve, but using the Wien displacement law one can estimate the minimum temperature of the target surface using Eq. (1):

$$\lambda_{max} = b/T \quad (1)$$

where $b \approx 2900$ μm K, the temperature of the hot graphite surface must be >390 °C.

Fig. 4 shows that this background is much lower in the case of air than in either argon or helium. As the thermal conductivity of the rare gases is greater than that of air one would expect better cooling in Ar and He, thus lower thermal background in rare gases than in air. This argument weakens the attribution of the background to a hot graphite surface, although one should consider that radiation processes in the plasmas are complex phenomena.

Another possible source of the background may be incandescence of carbon dust (soot) ablated by a laser pulse and heated by the rear side of this pulse or 100 ms later by the subsequent pulse. Laser induced incandescence (LII) of soot is a widely studied subject (e.g. Ref. [27]) but there exist no reports on infrared LII so far, so we have no reference material to use.

Finally the smooth background we observe could be due to a continuum of infrared spectra of a collection of various carbon molecules, but

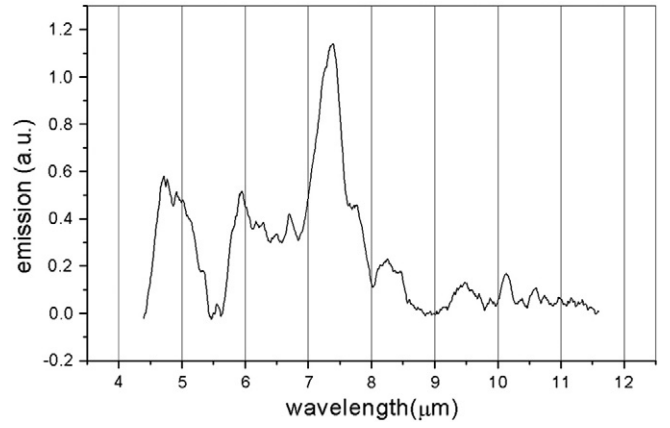

Fig. 7. Carbon plasma spectrum in argon between 4.4 and 11.5 μm, noise-filtered by a Welch filter, and spectral background corrected using 3rd-order polynomial fit to the base of the raw spectrum.

Table 1
Carbon chains C_5, C_6, C_7 and C_9 which have infrared active modes between 4.4 and 5.3 μm [21].

Electronic ground state symmetry	Carbon chain	Vibrational mode	Wave number (cm^{-1})	Wavelength (μm)
$^1\Sigma_g^+$	C_5	υ_3 (σ_u)	2169.44	4.609
$^3\Sigma_g^-$	C_6	υ_4 (σ_u)	1959.86	5.102
$^1\Sigma_g^+$	C_7	υ_4 (σ_u)	2138.32	4.676
$^1\Sigma_g^+$	C_9	υ_5 (σ_u)	2079.67	4.809

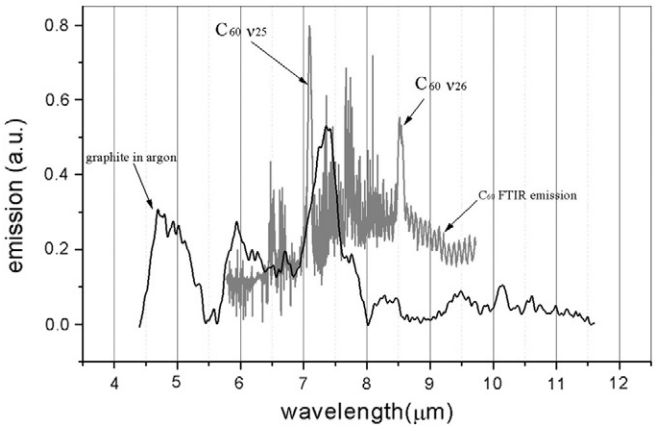

Fig. 8. Comparison of the present carbon plasma spectrum in argon (see Fig. 7) to the infrared emission spectrum of hot gas-phase C_{60} from Ref. [24]. Permission for using this spectrum was granted by Prof. Peter F. Bernath.

this is unlikely as tens of μs after the laser pulse ongoing plasma chemistry should result in a much smaller number of thermodynamically and kinetically preferred structures, thus a structured background.

5. Summary

We believe the present exploratory study provides a starting point for further experiments on infrared emission spectroscopy of laser induced carbon plasmas that would result in interesting new information about carbon clusters. Using a new MCT linear array detection system rapid measurements of infrared emission spectra of laser-induced plasmas have recently been reported [28]. This new technique renders the measurements of time-resolved carbon plasmas much easier (e.g. by reducing noise) than in our present slow scanning spectra that are also sample and background gas demanding ones. Important further steps can now be taken. One particular advance envisioned is simultaneous joint UV/visible and mid infrared LIB spectroscopy. Plasma physical parameters obtained from atomic lines in the UV/visible range would be significant help to establish the chemistry and excitation mechanisms at work in infrared LIBS and could significantly contribute to the understanding of the complex physical and chemical processes taking place in carbon plasmas.

Acknowledgements

The authors from Hampton University acknowledge financial support by the Army Research Office (ARO) through grant W911NF-12-1-0049 and the National Science Foundation through grant HRD-1131147.

L. Nemes acknowledges invitation from Professor A. Peter Snyder to give a talk on the present subject at Pittcon 2015, New Orleans in collaboration with the present authors. Financial travel and subsistence support from the Pittcon Organizing Committee is acknowledged.

References

[1] J. Mink, G. Keresztury, Appl. Spectrosc. 47 (1993) 1446–1451.
[2] G. Keresztury, J. Mink, J. Kristóf, Anal. Chem. 67 (1995) 3782–3787.
[3] P.F. Bernath, Annu. Rep. Prog. Chem., Sect. C 96 (2000) 177–224.
[4] G. Hancock, J.P. Sucksmith, J. Vac. Sci. Technol. A 13 (1995) 2945–2949.
[5] C.S.-C. Yang, E. Brown, U. Hommerich, S.B. Trivedi, A.P. Snyder and A.C. Samuels, Report 01 Nov. 2006, Battelle Eastern Science and Technology Center, Aberdeen, MD 21001.
[6] C.S.-C. Yang, E. Brown, U. Hommerich, S.B. Trivedi, A.P. Snyder, A.C. Samuels, Appl. Spectrosc. 61 (2007) 321–326.
[7] C.S.-C. Yang, E. Brown, U. Hommerich, S.B. Trivedi, A.C. Samuels, A.P. Snyder, Appl. Spectrosc. 62 (2008) 714–716.
[8] C.S.-C. Yang, E. Brown, U. Hommerich, S.B. Trivedi, A.C. Samuels, A.P. Snyder, Spectroscopy 23 (2008) 29.
[9] O. Oyebola, U. Hommerich, E. Brown, C.S.-C. Yang, S.B. Trivedi, A.C. Samuels, A.P. Snyder, Photonic Lett. Poland 3 (2011) 171–174.
[10] C.S.-C. Yang, E. Brown, U. Hommerich, F. Jin, S.B. Trivedi, A.C. Samuels, A.P. Snyder, Appl. Spectrosc. 66 (2012) 1397–1402.
[11] C.S.-C. Yang, E. Brown, E. Kumi-Barimah, U. Hommerich, F. Jin, S.B. Trivedi, A.C. Samuels, A.P. Snyder, Appl. Spectrosc. 68 (2014) 226–231.
[12] H.W. Kroto, J.R. Heath, S.C. O'Brien, R.F. Curl, R.E. Smalley, Nature 318 (1985) 162–163.
[13] W. Kraetschmer, L.D. Lamb, K. Fostiropoulos, D.R. Huffman, Nature 347 (1990) 354–358.
[14] http://www.nobelprize.org/nobel_prizes/chemistry/laureates/1996/.
[15] L. Nemes, S. Irle (Eds.), Spectroscopy, Dynamics and Molecular Theory of Carbon Plasmas and Vapors, World Scientific, Singapore, 2011.
[16] K. Sasaki, in: L. Nemes, S. Irle (Eds.), Spectroscopic Studies on Laser-Produced Carbon Vapor, World Scientific, Singapore 2011, pp. 55–76.
[17] P. Ehrenfreund, B.H. Foing, Science 329 (2010) 159–1160.
[18] http://astro.dur.ac.uk/~pdraper/splat/splat-vo/splat-vo.html.
[19] A. Kramida, Y. Ralchenko, J. Reader, NIST ASD Team, NIST Atomic Spectra Database, 2014 (version 5.2).
[20] G. Herzberg, The Spectra and Structures of Simple Free Radicals, Cornell University Press, New York, 1971.
[21] A. van Orden, R.J. Saykally, Chem. Rev. 98 (1998) 2313–2357.
[22] B. Chase, N. Heron, E. Holler, J. Phys. Chem. 96 (1992) 4262–4266.
[23] C.I. Frum, R. Engleman Jr., H.G. Hedderich, P.F. Bernath, L.D. Lamb, D.R. Huffman, Chem. Phys. Lett. 176 (1991) 504–508.
[24] L. Nemes, R.S. Ram, P.F. Bernath, F.A. Tinker, M.C. Zumwalt, L.D. Lamb, D.R. Huffman, Chem. Phys. Lett. 218 (1994) 295–303.
[25] A.G.G.M. Tielens, Annu. Rev. Astron. Astrophys. 46 (2008) 289–337.
[26] C.J. Mackie, E. Peeters, C.W. Bauschlicher Jr., J. Cami, Astrophys. J. 799 (2015) 1–11.
[27] F. Goulay, L. Nemes, P.E. Schrader, H.A. Michelsen, Mol. Phys. 108 (2010) 1013–1025.
[28] C.S.-C. Yang, E. Brown, E. Kumi-Barimah, U. Hommerich, F. Jin, Y. Jia, S.B. Trivedi, A.I. D'Souza, E.A. Decuir Jr., P.S. Wijewarnasuriya, A.C. Samuels, Appl. Opt. 54 (2015) 9695–9702.